AD-A046 258 NATIONAL BUREAU OF STANDARDS WASHINGTON D C INST FO--ETC F/G 20/4
AN EXPERIMENTAL STUDY OF TRANSITION ON BLUNT BODIES. PART I.(U)
JUL 77 G CHRISTOPH, K D TIDSTROM

UNCLASSIFIED NBSIR-77-1258 NL

1 OF 1
ADA
046258

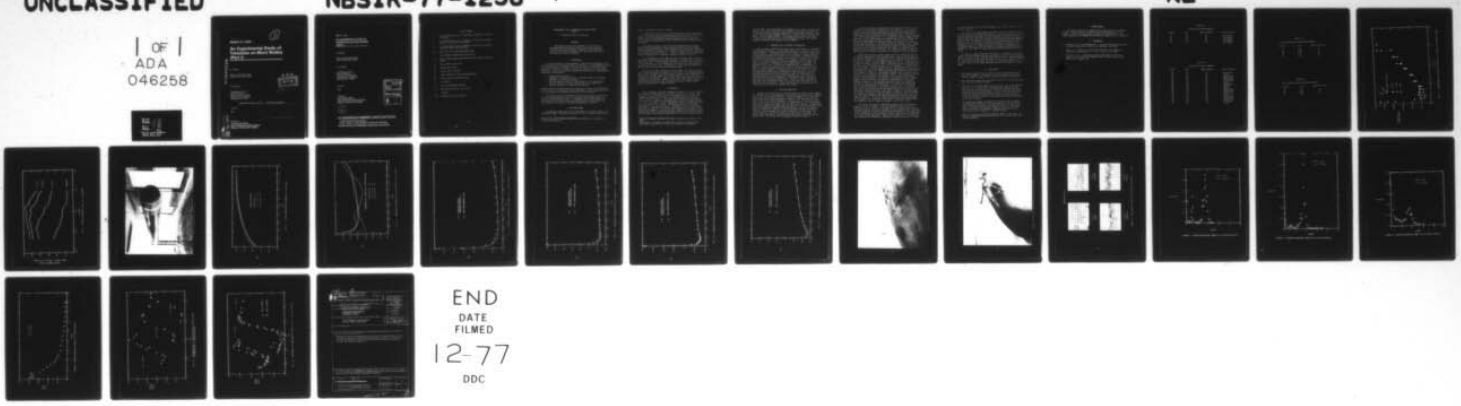

END
DATE
FILMED
12-77
DDC

NBSIR 77-1258

An Experimental Study of Transition on Blunt Bodies (Part I)

G. Christoph

Naval Undersea Systems Center
Newport, Rhode Island 02840

K. D. Tidstrom

Fluid Mechanics Section
Mechanics Division
Institute for Basic Standards
National Bureau of Standards
Washington, D.C. 20234

APPROVED FOR PUBLIC RELEASE: DISTRIBUTION UNLIMITED

July 1977

Final

Prepared for
Commanding Officer
Naval Underwater Systems Center
Newport, Rhode Island 02840

NBSIR 77-1258

AN EXPERIMENTAL STUDY OF TRANSITION ON BLUNT BODIES (PART I)

G. Christoph

Naval Undersea Systems Center
Newport, Rhode Island 02840

K. D. Tidstrom

Fluid Mechanics Section
Mechanics Division
Institute for Basic Standards
National Bureau of Standards
Washington, D.C. 20234

July 1977

Final

Prepared for
Commanding Officer
Naval Underwater Systems Center
Newport, Rhode Island 02840

U.S. DEPARTMENT OF COMMERCE, Juanita M. Kreps, *Secretary*

Dr. Sidney Harman, *Under Secretary*

Jordan J. Baruch, *Assistant Secretary for Science and Technology*

NATIONAL BUREAU OF STANDARDS, Ernest Ambler, *Acting Director*

LIST OF SYMBOLS

u'	*root-mean-square* value of longitudinal component of velocity fluctuation
v'	root-mean-square value of component of velocity fluctuation lateral to the mean flow direction
w'	root-mean-square value of component of velocity fluctuation vertical to mean flow direction
U_o	mean velocity of flow approaching model
x	axial distance downstream from nose face
x_t	axial distance downstream from nose face at which transition begins
y	nose radius at position x
R	maximum nose radius
P_s	surface static pressure
P_o	static pressure in flow approaching model
P_T	total pressure from surface tube
ρ	air density
q	free-stream dynamic pressure
C_P	pressure coefficient, $(P_s - P_o)/q$
n	frequency
$F(n)$	normalized spectral function

EXPERIMENTAL STUDY OF TRANSITION ON BLUNT BODIES (PART I)

G. Christoph[1] and K. D. Tidstrom

ABSTRACT

Experimental results are presented for the effects of Reynolds number and angle-of-attack on the static pressure distribution and the location of laminar to turbulent transition for the flow over several blunt noseforms; comparisons are made with analytical methods.

1. INTRODUCTION

It was the purpose of this experiment to gain further knowledge of the flow processes over blunt-nosed bodies of revolution. An experimental program was outlined which was intended to discern the effects of Reynolds number, background turbulence, and angle-of-attack on transition for several blunt noseforms. It was felt that the program objectives would be accomplished by taking the following data:

1. Static pressure profiles.
2. Dependence of transition region on Reynolds number, freestream turbulence, and angle-of-attack.
3. Relative spectral content of disturbances, at a fixed position from the surface for before, during, and end of transition.
4. Spatial uniformity of transition around noses.

Relating analytics and the above data would allow for an accurate prediction of the location of transition on blunt axisymmetric bodies, and would serve as a starting point for modeling transition as a noise source.

The transition results presented in this report, except for the effect of free-stream turbulence, are for two different blunt-nosed bodies of revolution identified as A and B. A subsequent report will present data on transition for the blunt-nose body of revolution identified as W, as well as data on the effect of free-stream turbulence on body B.

2. NBS WIND TUNNEL

The NBS wind tunnel used for this experiment is a closed circuit, low turbulence tunnel. The test section has a 1.22 x 1.52 meters cross-section,

---

[1]Previously at Naval Undersea Systems Center, Newport, RI; presently at Sun Ship, Chester, PA.

and has a maximum air speed of 76 m/sec.

A hemispherical nose Pitot-static tube was used to make longitudinal static pressure and velocity measurements in the test section of the wind tunnel. The blunt-nosed body was positioned in the test section in a region where the longitudinal pressure gradient was approximately zero. In this region, the velocity did not vary by more than 0.7 percent across the tunnel.

The turbulence level of the wind tunnel was measured by constant current hot-wire anemometry using a special vibration isolation mount. The root-mean-square values of the longitudinal and transverse components of the turbulent fluctuations, u', v' and w', respectively, as a function of air speed are shown in figure 1. Such low values of free-stream turbulence are exemplary for wind tunnel studies of transition [1,2].[2]

Noise measurements of the NBS wind tunnel were made with a General Radio type 1560P5 microphone[3] which was fed to a General Radio type 1551-C sound level meter. The microphone was mounted through a hole in the wall of the wind tunnel in such a manner that the face of the microphone was parallel to the tunnel wall. In addition, a wind screen was placed over the microphone face and flush with the tunnel wall.

The noise data were collected on tape at NBS for various air speeds and two angles-of-attack (0° and +3°) of the model. The one-third octave spectra were obtained at the Naval Undersea Systems Center (NUSC) by playing back the recorded signals to a General Radio type 1521, real time, one-third octave analyzer. Figure 2 gives the sound pressure level versus frequency for several air speeds with the model at 0° angle-of-attack. No noticeable differences were obtained in the sound pressure levels when the model was at 3° angle-of-attack.

3. TEST MODELS

Three aluminum, flat-faced axisymmetric models, 20.32 cm in diameter, were machined at NUSC, Newport. The models are about 30 cm long, and screw into a long cylinder, 20.32 cm in diameter and 1.5 m long. The assembled configuration is held by a sting and mounted to the tunnel floor as shown in figure 3. Each model has 24-30 pressure taps placed so as to provide static pressure measurements from the stagnation region to an $x/R = 1.8$, where x is the longitudinal distance from the nose, and R is the radius of the cylinder. Pressure taps were also provided to align model at zero angle-of-attack. On Model A, except for the alignment taps, all pressure taps were located along the top generator along the plane of symmetry. The pressure taps on Model B were located as for Model A except that additional taps were located near the nose at generators 90° apart and so spaced longitudinally as to give a greater density

[2] Figures in brackets represent literature references at the end of this paper.

[3] Brand names of equipment are used solely to provide a reference for performance characteristics and do not represent an endorsement.

of measurement. The three models are designated A, B, and W. As seen from figure 4, all model contours are quite similar, but as seen from figure 5, the theoretical static pressure distributions are markedly different. Model A has a broad pressure minimum, Model B has a sharper pressure minimum, and Model W has two pressure minima. The pressure distribution curves shown in figure 5 were generated by the Douglas-Neumann potential flow computer program (developed by the Douglas Aircraft Company).

4. MEASURED STATIC PRESSURE DISTRIBUTIONS

Plastic tubing connected the pressure taps on the model to a scanivalve mounted inside the model. A single tube connected the scanivalve to an inclined manometer. A hemispherical nose Pitot-static tube with a right-angle-stem was used to obtain the reference static pressure at a position about 0.5 meters downstream from the flat face of the models. Measured pressure distributions at a speed of 38 m/sec are compared in figures 6 and 7 to the theoretical distributions for Model A at 0° angle-of-attack and for Model B at -3°, 0°, and +3° angle-of-attack. Measurements at a +3° angle-of-attack correspond to measurements on the leeward side of the model. The agreement is very good. Pressure distributions were also measured at a speed of 76 m/sec for Model A, and at speeds of 58 m/sec and 76 m/sec for Model B. These pressure distributions, within the experimental accuracy were essentially identical to those shown in figures 6 and 7. The small differences observed between the theoretical and experimental pressure distributions may be due to the possibility that the coordinates of the machined models are not precisely the coordinates that were initially specified and very slight differences in the computer input coordinates will affect the theoretical predictions. Another possible reason may be the effect that the boundary layers on the wind tunnel walls have on the model pressure distribution. It should be noted that the theoretical calculations do not account for boundary layer growth.

5. LOCATING TRANSITION

Inasmuch as the detection of transition generally requires some judgment in interpretation, it was desirable to use several methods in order to assess the accuracy in locating transition. Hot-wire anemometry and a total-head surface tube were both used to detect transition. The hot-wire probe was constructed of two needles cemented to a lucite sled. The sled was 1.59 cm long, 1.11 cm wide, and 0.32 cm thick. A platinum wire, 1.27 μm in diameter and 0.058 cm long was attached across the tips of the needles. Spring tension held the sled against the model nose, and the distance of the wire above the surface was adjusted by repositioning the needles. Usually, the distance above the surface was 0.025 cm. The hot-wire probe and sled are shown in figure 8. The total-head surface tube consisted of a nickel tube, 1 mm outside diameter, flattened at the end to form a 0.0127 cm opening. A static tube, also made of 1 mm nickel tubing was mounted 0.635 cm from the surface tube. The surface tube arrangement is shown in figure 9.

Locating transition by observing and interpreting the hot-wire signal displayed on an oscilloscope proved to be very difficult. The laminar boundary layer oscillation frequencies (in the adverse pressure gradient region) were found to have very high frequencies and were difficult to distinguish from the frequencies in the transition zone. The narrow extent of the transition region (only 3 to 6 centimeters) further complicated the situation. It was obvious when the boundary layer was fully laminar and when the boundary layer was fully turbulent, but the location of the transition from laminar to turbulent flow was not obvious. By filtering out the lower frequencies, the interpretation was somewhat easier. Figure 10 displays oscillograms illustrating the presence of laminar boundary layer oscillations and the transition from laminar to turbulent flow on Model B for an air speed of 38 m/sec. The signal amplitudes in figure 9 were adjusted for illustration and bear no relation to actual amplitudes.

Another method used to locate transition was to measure the spectra of velocity fluctuations in the boundary layer. Spectra illustrative of the spectral behavior of velocity fluctuations associated with transition are shown in figures 11-14 for Model B at an air speed of 58 m/sec and a 0° angle-of-attack. The measurements shown were made in the boundary layer at 0.025 cm from the surface, and are presented in terms of the spectral function, F(n), the energy per unit cycle at frequency, n, normalized with the total energy. The flow characterized by the spectrum at $x/R = 1.71$ is regarded as still being laminar with the peaked behavior of the spectrum indicating the presence of laminar boundary layer oscillations as in the oscillograms of figure 10. The laminar boundary layer oscillations are a product of the experimental environment coupled to the instability process and more than one peak in the spectrum can occur, particularly in an adverse pressure gradient. For example, the frequencies of the laminar boundary layer oscillations increase with speed and at 76 m/sec the dominant frequency in the spectrum just before transition is 6200 Hz. At 38 m/sec there are two dominant peaks in the spectrum, 1800 Hz and 2150 Hz, at the beginning of transition. At 76 m/sec it was observed that the spectral content of the laminar boundary layer oscillations also varies with angle-of-attack with higher frequencies occurring in the more severe pressure gradient. This was not evident at the lower speed of 38 m/sec. Within the transition region the spectral content broadens to include more energy at lower and higher frequencies and at $x/R = 2.34$ the flow is fully turbulent as characterized by the continuous spectrum shown in figure 14. It is the initial broadening of the spectrum which is considered to be indicative of the onset of transition, and for the case shown the onset of transition appears to be at $x/R = 1.84$.

The surface tube method of detecting transition is illustrated in figure 15 in which results at three air speeds for Model B, at a +3° angle-of-attack, are shown. It is seen that for a fixed position above the model surface, the velocity decreases in the laminar region, increases rapidly through the transition region, and then decreases, once again, due to the growing layer in the turbulent region. There was no direct evidence of a strong steady separation. However, the possibility of a transition associated with an intermittent separation cannot be ruled out. In order

to determine whether the latter does indeed occur, a more extensive effort would be required.

All three of the above methods were used to locate transition but not all three were used for each test condition. The results obtained together with the method of detecting transition are given in tables 1a and 1b. It is seen from tests made under the same conditions with different methods of detection that the location of transition was reasonably well-determined to within ± 0.1R. It should be noted that of the three methods the surface tube was felt to be the most convenient and easiest to interpret. The transition location for Models A and B for various wind speeds and at a 0° angle-of-attack were also calculated by the Mangler transformed Michel method [3]. The results of these calculations are presented in tables 2a and 2b.

In order to assess the spatial uniformity of transition, total-head surface tube measurements were made for Model B at the 90° (top) and 180° (side) positions, as one views the model from the front. These measurements were made at wind speeds of 38 m/sec and 76 m/sec for an angle-of-attack of 0°. The results are presented in figure 16. Transition appears to be spatially uniform at the lower speed and slightly nonuniform at the higher speed.

6. CONCLUSIONS

1. The measured and theoretical static pressure distributions were in excellent agreement. This means that one can machine blunt nosed models accurately enough to give a predicted pressure distribution.

2. The energy associated with the laminar oscillations could be detected well into the transition region.

3. Transition on the blunt bodies under test was not as easily identifiable as on a flat plate, that is, sudden large jumps in the mean velocity close to the surface associated with turbulent spots were not observed on the blunt bodies. If the fact that the transition region is noisier than the turbulent region on a flat plate is due to abrupt increases in the mean velocity, then perhaps on blunt bodies the flow noise levels in the transition and turbulent regions do not differ greatly.

4. At low Reynolds numbers, transition was uniform around the models. At higher Reynolds numbers, transition appeared to be nonuniform. This nonuniformity has also been observed in previous work at NBS and in flow visualization tests conducted recently at the National Physical Laboratory in Teddington, England, and appeared to be associated with the formation of turbulent wedges.

5. Of all the transition prediction methods compared to the data, the Mangler transformed Michel method was the only one which gave satisfactory agreement.

7. ACKNOWLEDGMENT

The authors would like to express their appreciation to D. Quadrini of NUSC for his assistance in making the noise measurements, and L. M. Sargent of NBS for his assistance in taking and compiling data. The authors gratefully acknowledge the interest and support of P. S. Klebanoff.

8. REFERENCES

1. Schubauer, G. B. and Skramstad, H. K., *Laminar Boundary Layer Oscillations and Transition on a Flat Plate*, NACA Rept. 909, 1948.

2. Wells, C. S., *Effects of Free Stream Turbulence on Boundary-Layer Transition*, AIAA Journal, vol. 5, no. 1, pp. 172-174, 1967.

3. Granville, P. S., *Comparison of Existing Methods for Predicting Transition from Laminar to Turbulent Flow on Bodies of Revolution*, NSRDC TN 111, August 1968.

Table 1(a)

Transition Location on Model A

U_o(m/s)	x_t/R	Angle-of-Attack	Detection Method
23	2.5	0°	Oscillogram
30	2.2	0°	Oscillogram
38	2.1	0°	Oscillogram
46	1.9	0°	Oscillogram
76	1.8	0°	Oscillogram

Table 1(b)

Transition Location on Model B

U_o(m/s)	x_t/R	Angle-of-Attack	Detection Method
38	2.1	0°	Oscillogram
38	2.1	0°	Spectra
38	2.0	0°	Surface-tube
38	2.0	+1°	Oscillogram
38	1.8	+3°	Oscillogram
38	1.7	+3°	Surface-tube
38	1.6	+3°	Spectra
38	2.2	-1°	Oscillogram
38	2.3	-3°	Spectra
58	1.8	0°	Spectra
58	1.8	0°	Surface-tube
58	1.1	+3°	Surface-tube
76	1.3	0°	Oscillogram
76	1.2	0°	Spectra
76	1.2	0°	Surface-tube
76	1.2	+1°	Oscillogram
76	0.6	+3°	Surface-tube
76	1.7	-1°	Oscillogram
76	1.9	-3°	Spectra

Table 2(a)

Calculated Transition Location on Model A

U_o (m/s)	x_t/R	Angle-of-Attack
23	2.25	0°
30	2.00	0°
38	1.85	0°
46	1.75	0°
76	1.52	0°

Table 2(b)

Calculated Transition Location on Model B

U_o (m/s)	x_t/R	Angle-of-Attack
38	1.52	0°
58	1.20	0°
76	0.95	0°

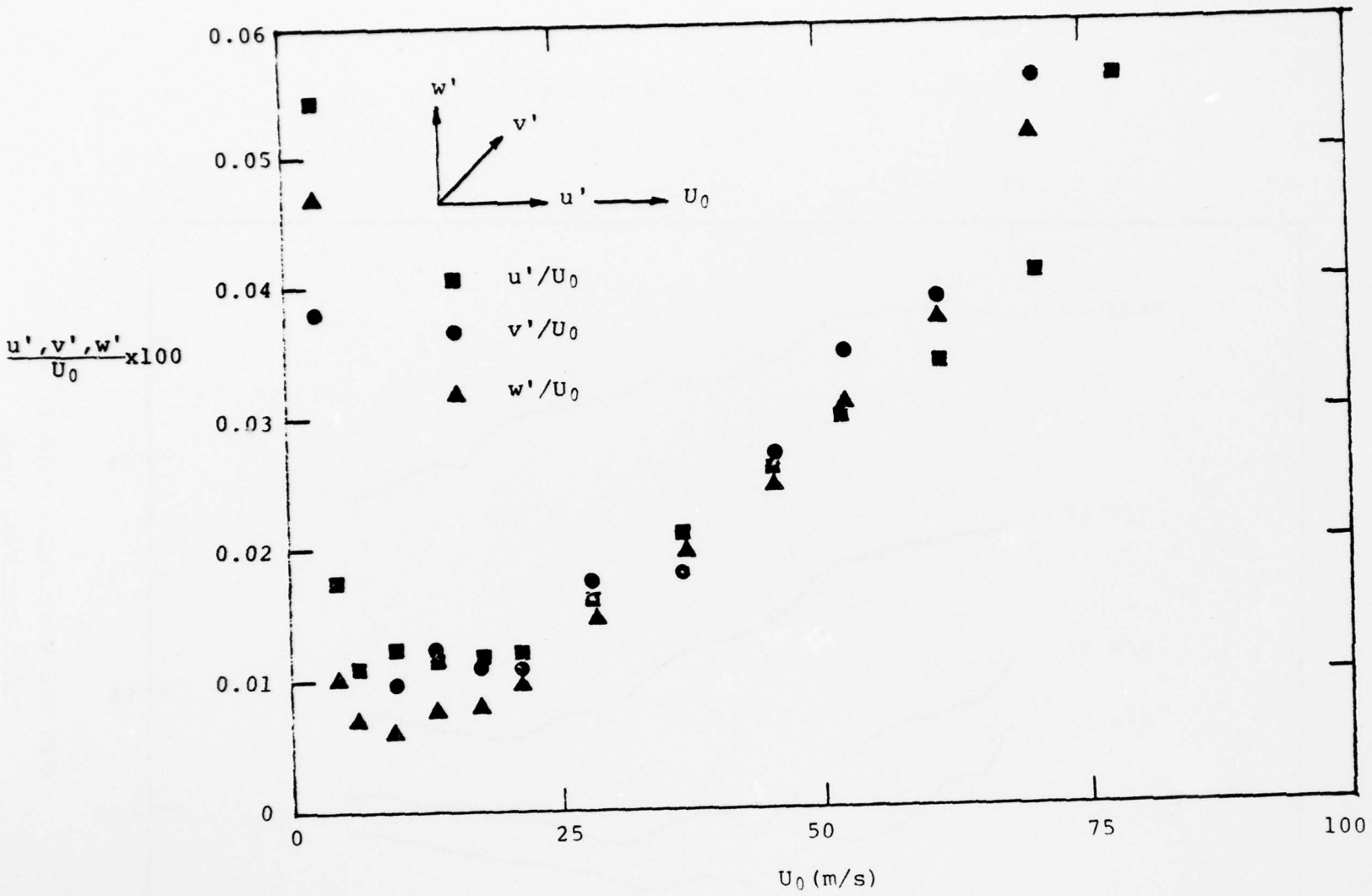

FIG. 1. FREESTREAM TURBULENCE LEVELS VS. SPEED IN NBS WIND TUNNEL

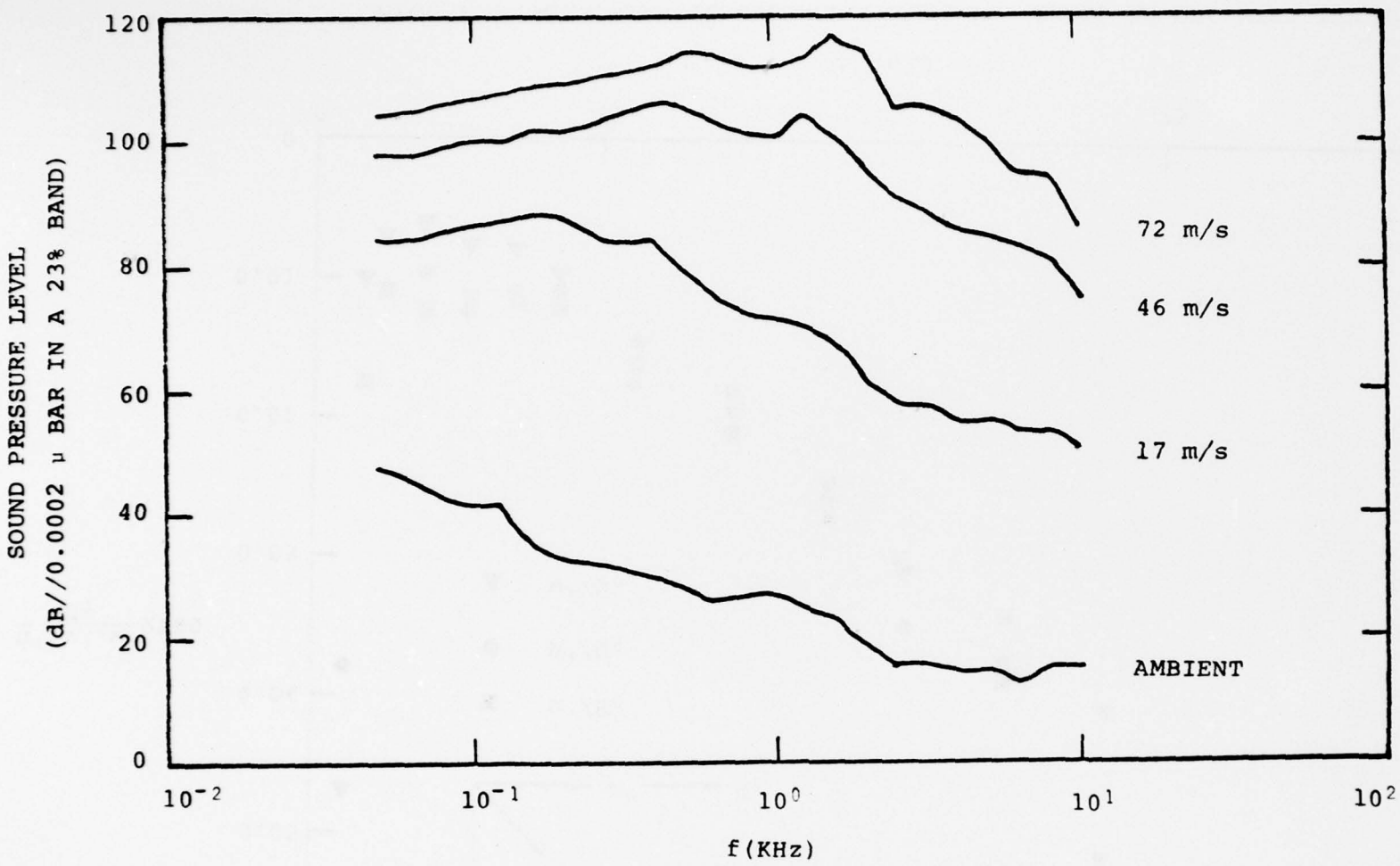

FIG. 2. SOUND PRESSURE LEVEL VS. FREQUENCY

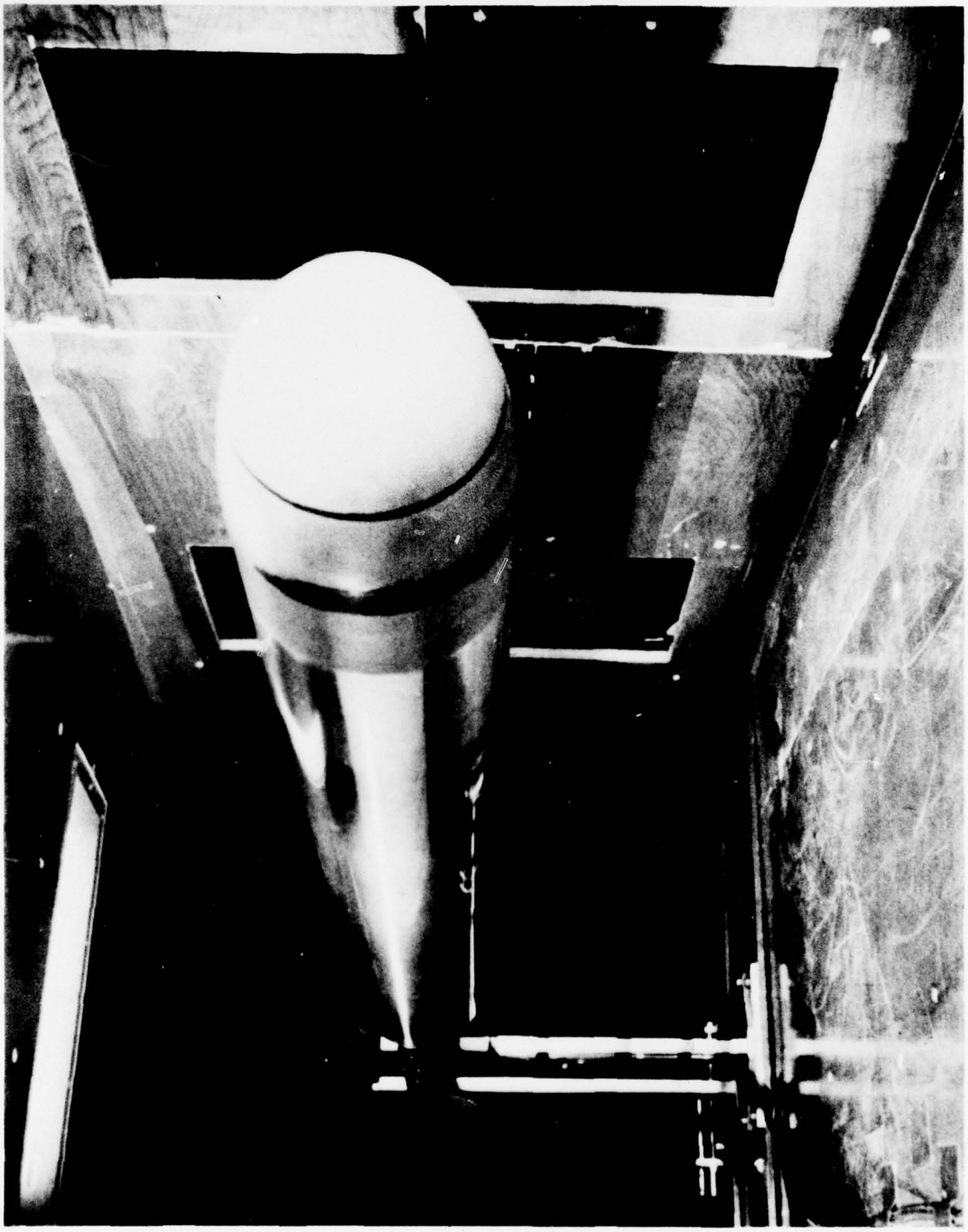

FIGURE 3. ASSEMBLED MODEL IN WIND TUNNEL

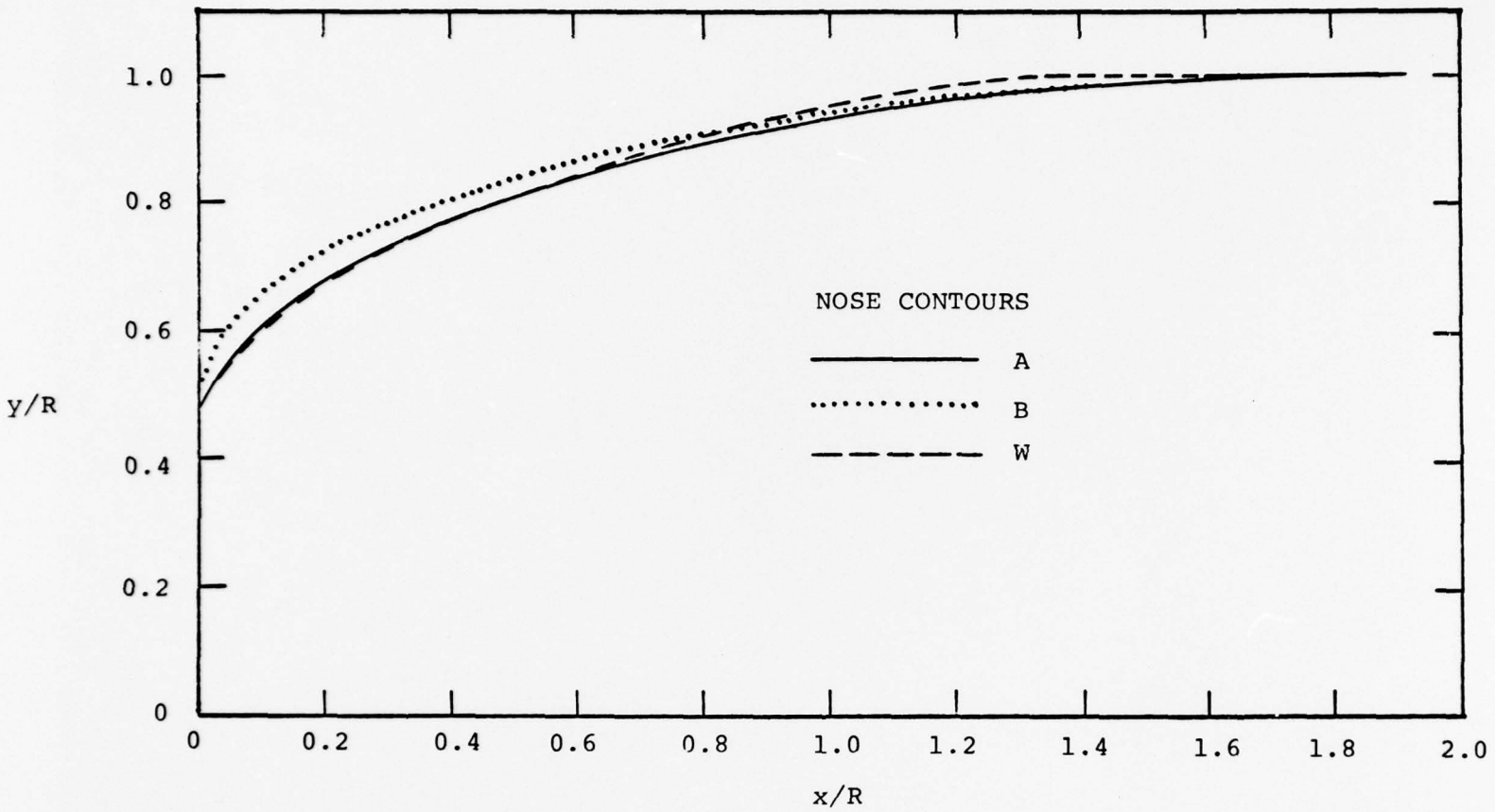

FIG. 4. NOSE CONTOURS FOR MODELS A, B, AND W

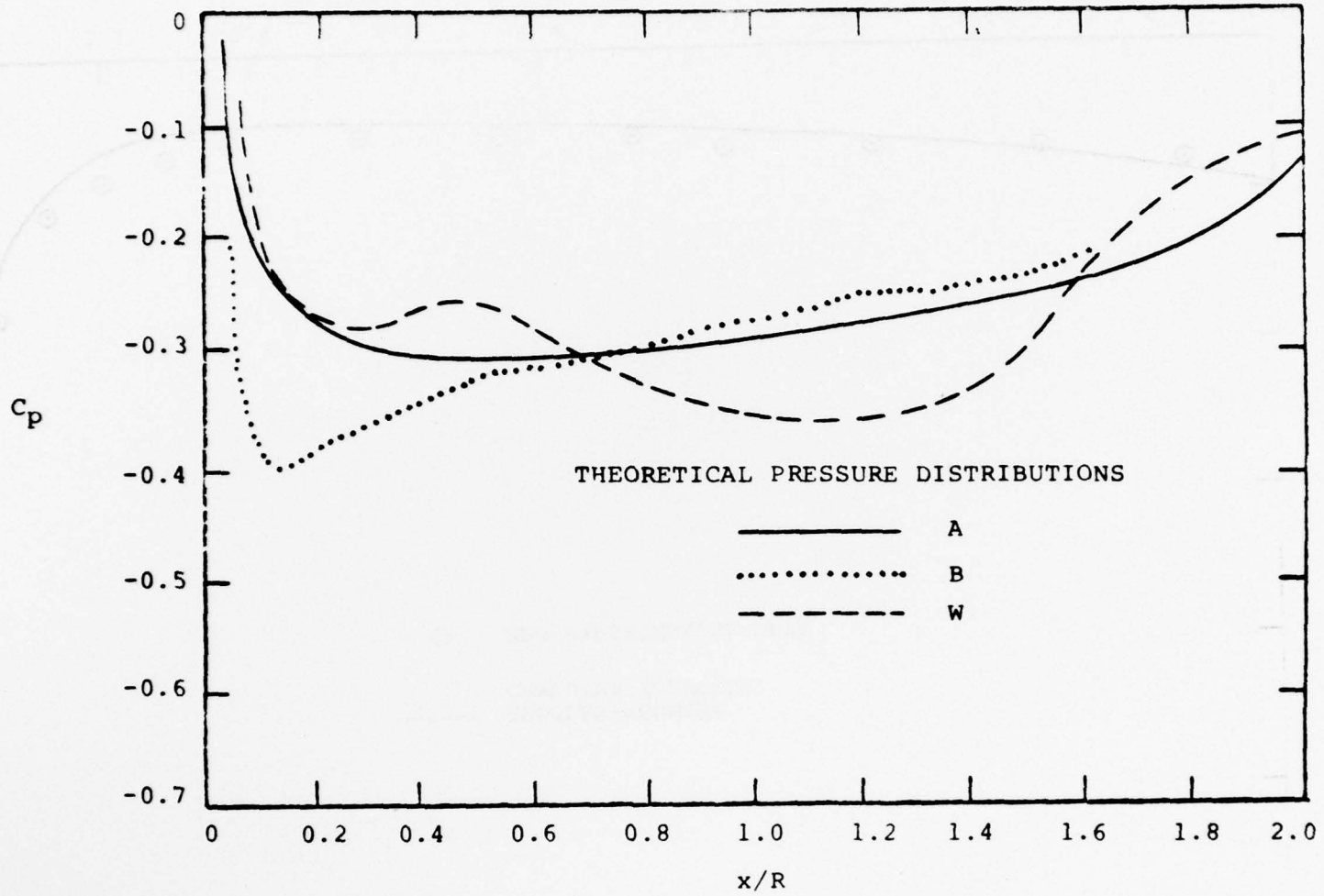

FIG. 5. PRESSURE DISTRIBUTIONS FOR MODELS A, B, AND W

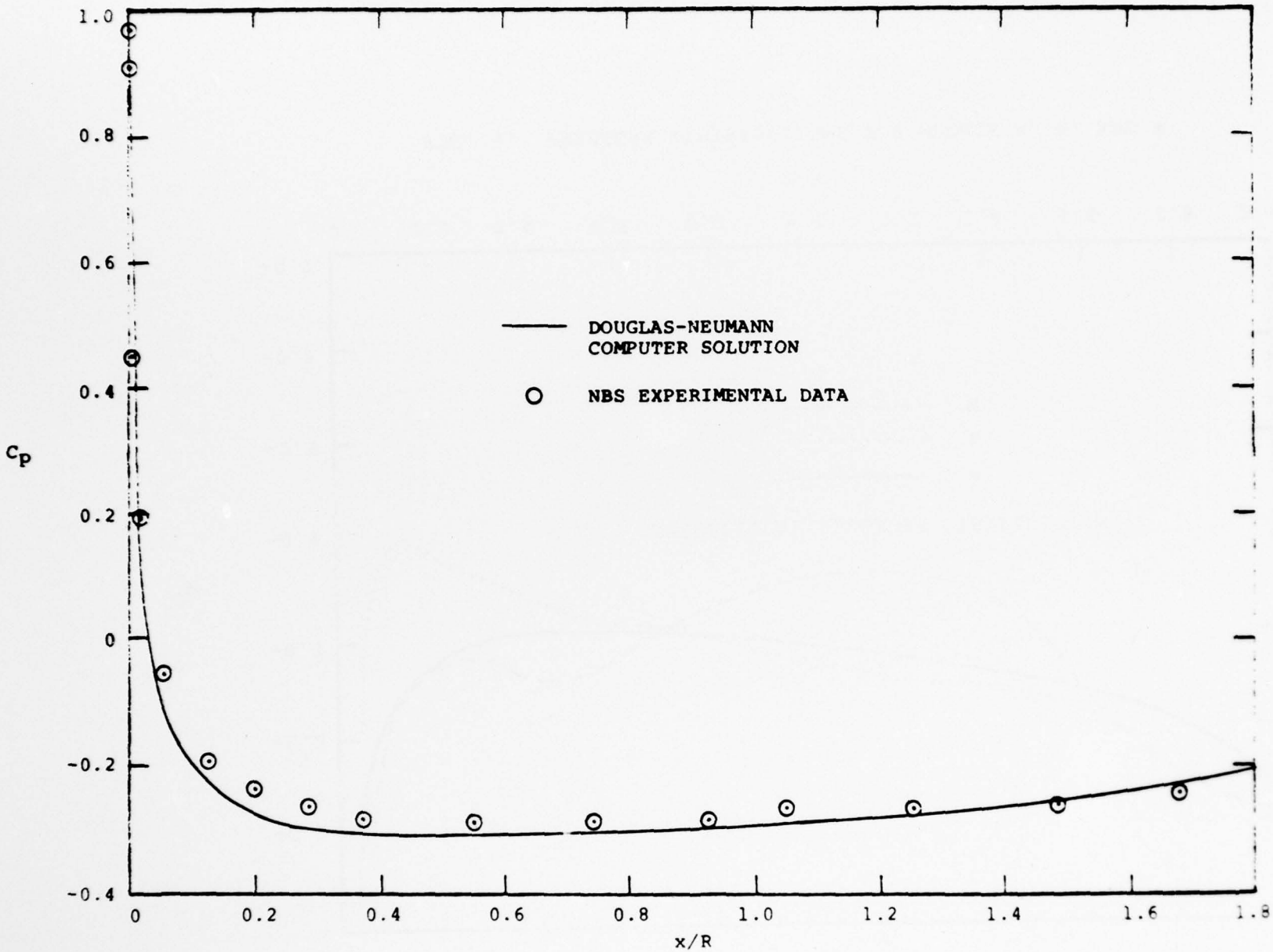

FIG. 6. PRESSURE DISTRIBUTION FOR MODEL A AT 0° ANGLE-OF-ATTACK

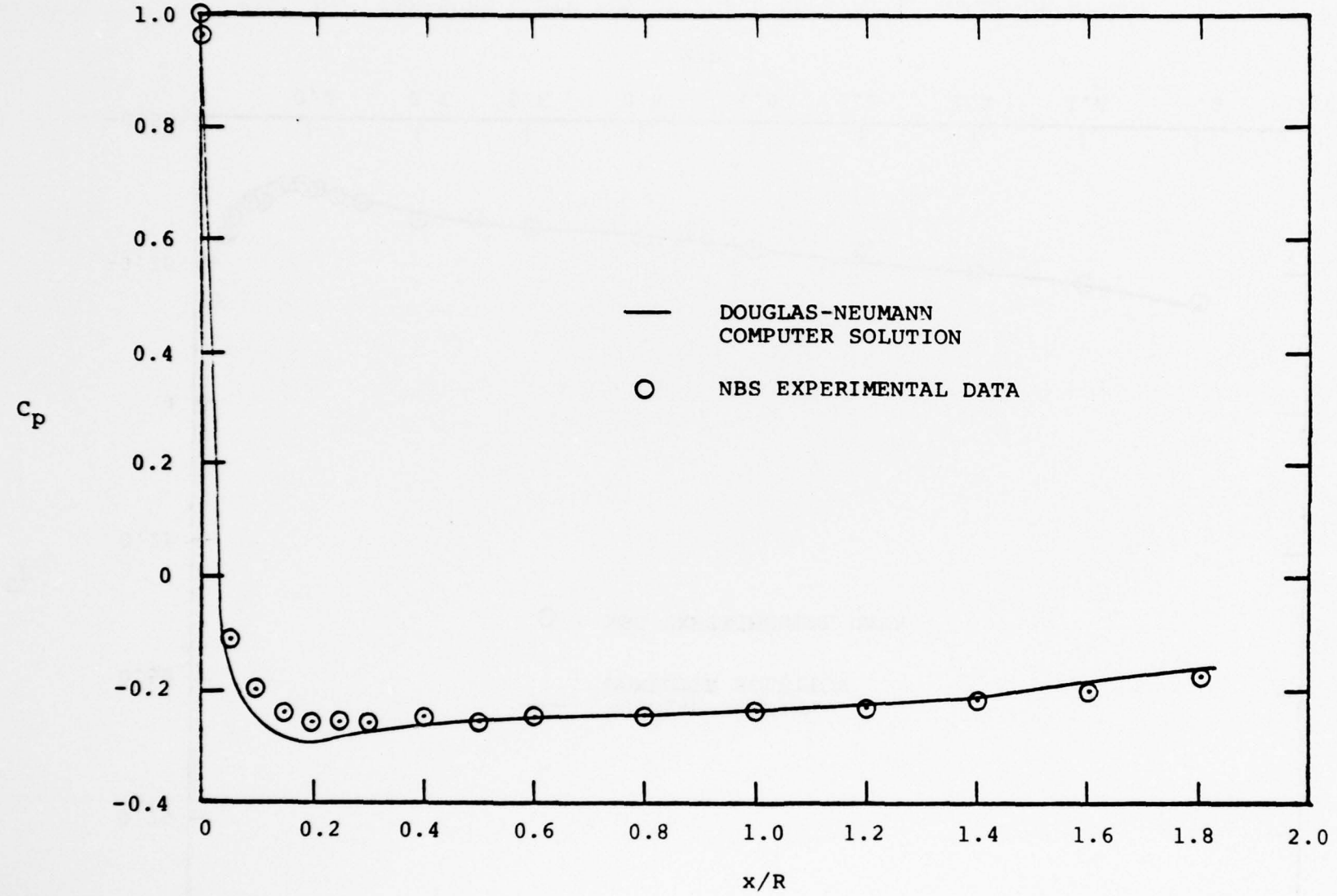

FIG. 7a. PRESSURE DISTRIBUTION FOR B NOSE AT -3° ANGLE-OF-ATTACK

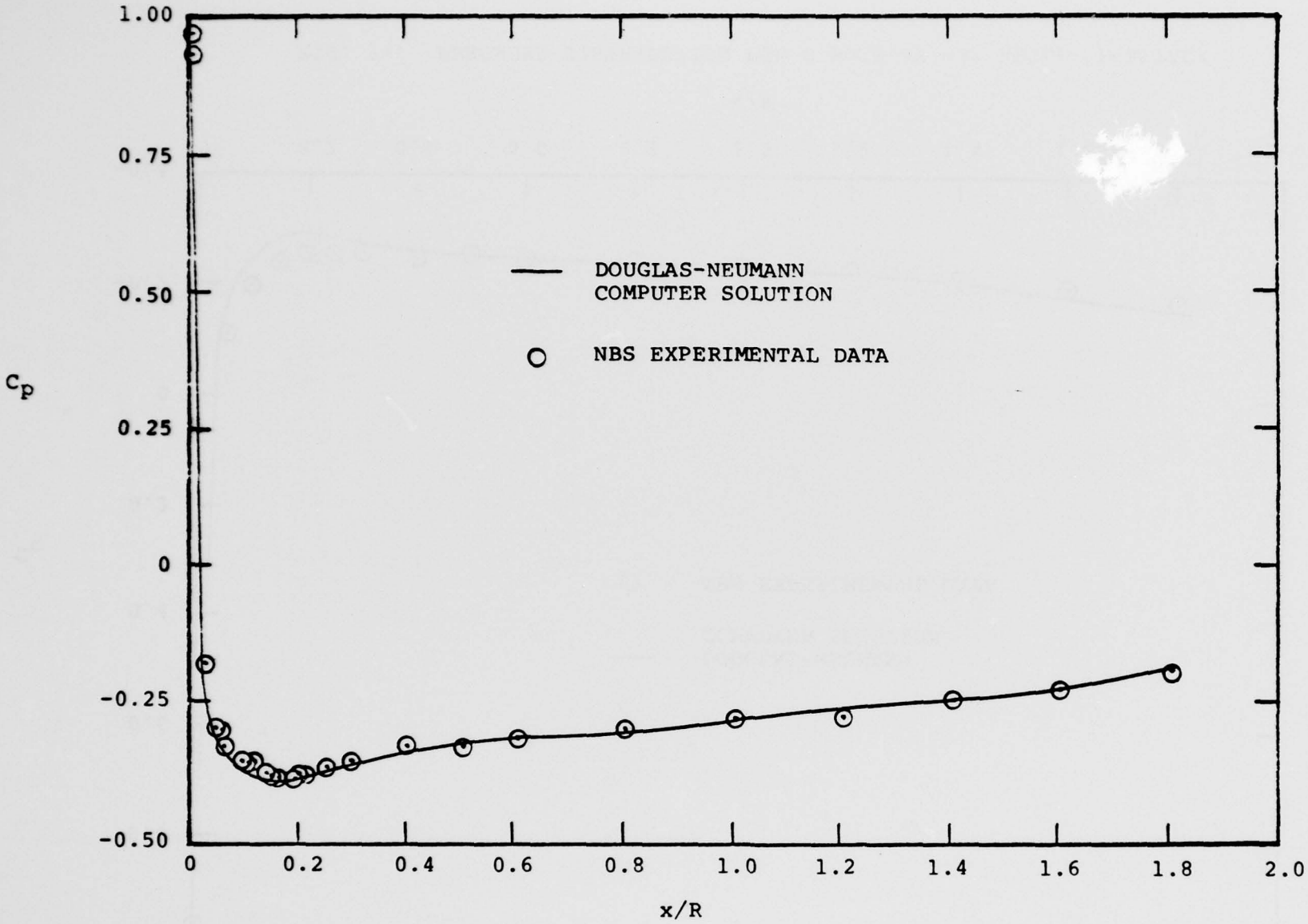

FIG. 7b. PRESSURE DISTRIBUTION FOR B NOSE AT 0° ANGLE-OF-ATTACK

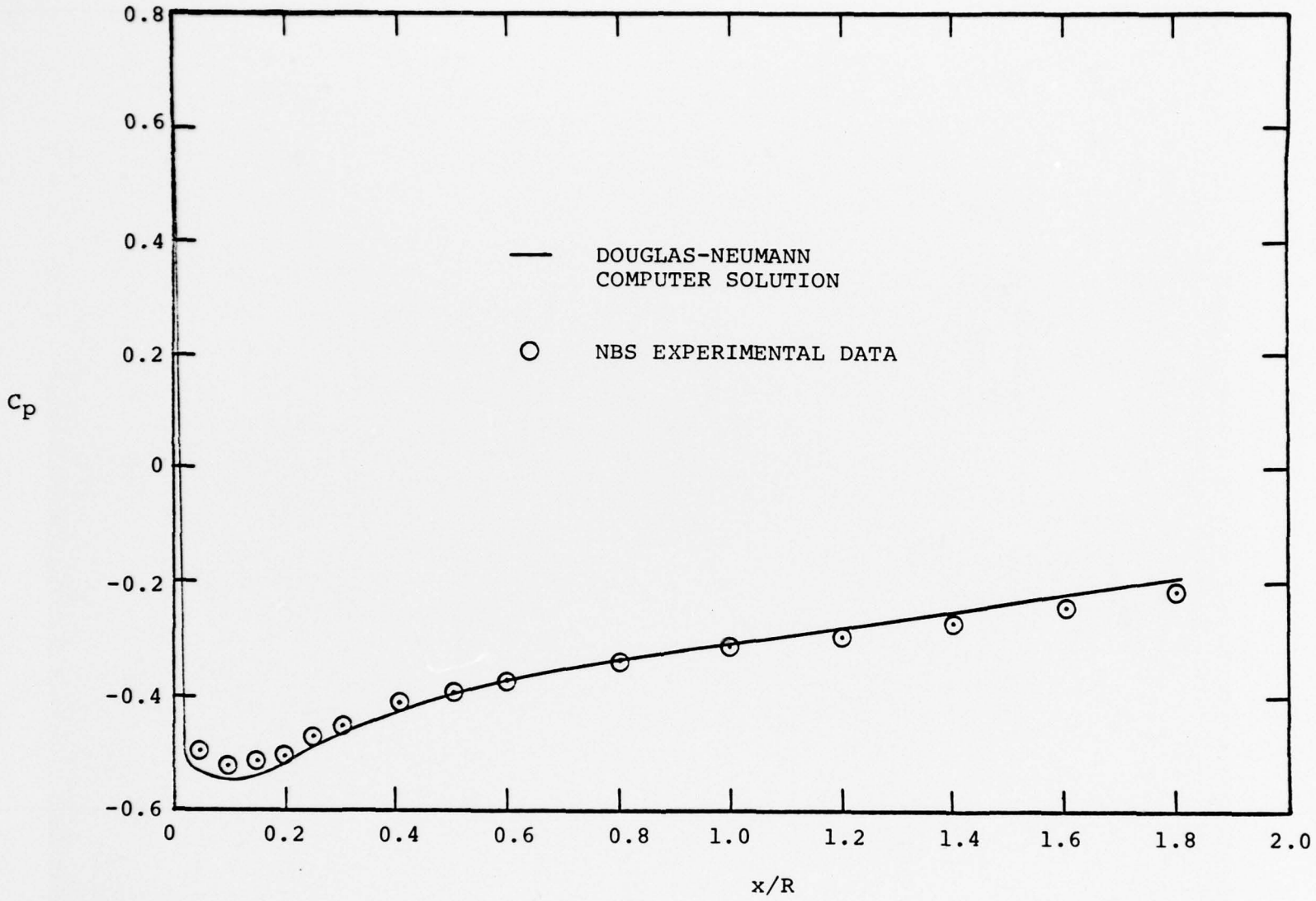

FIG. 7c. PRESSURE DISTRIBUTION FOR B NOSE AT +3° ANGLE-OF-ATTACK

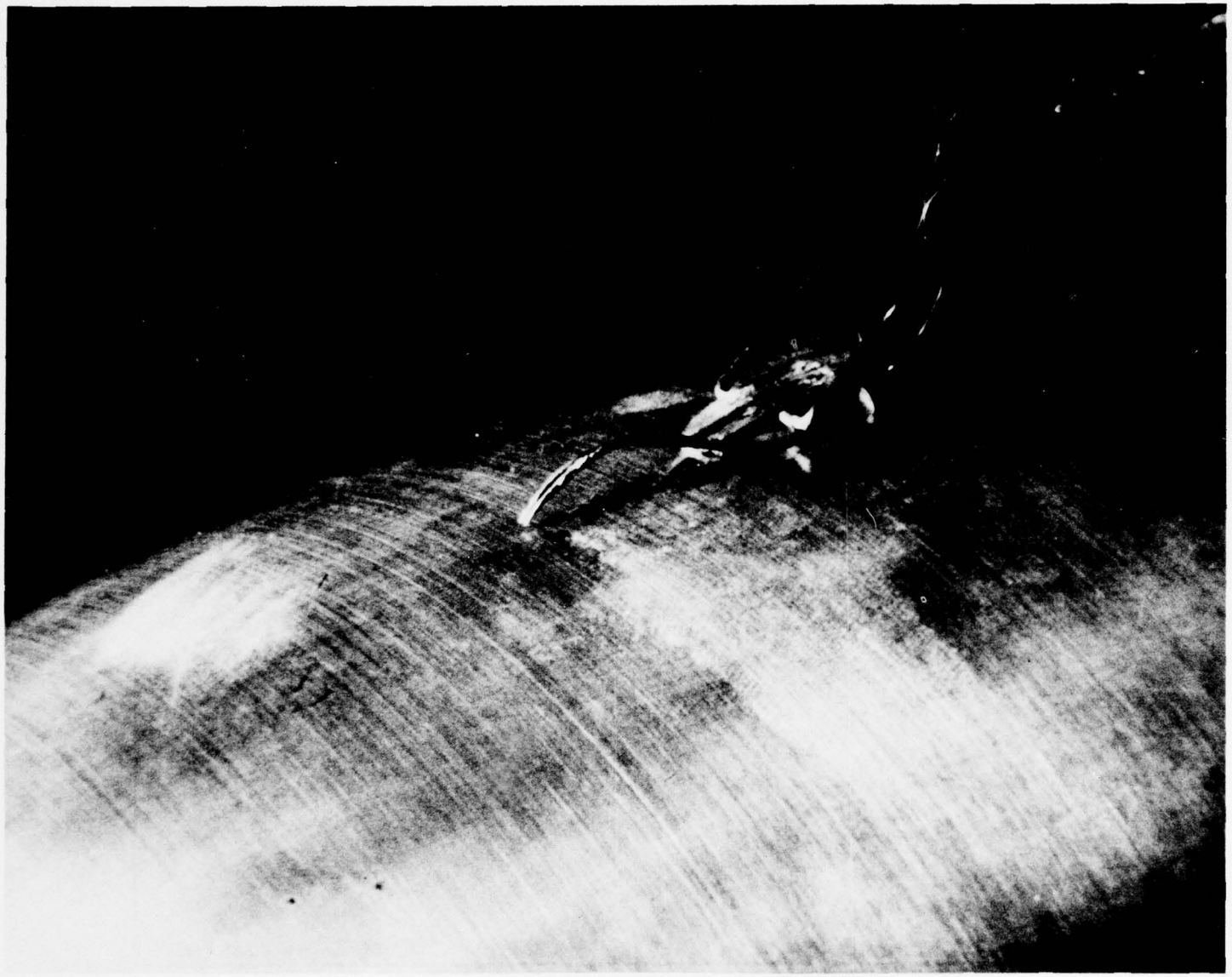

FIGURE 8. HOT-WIRE PROBE AND SLED FOR DETECTING TRANSITION

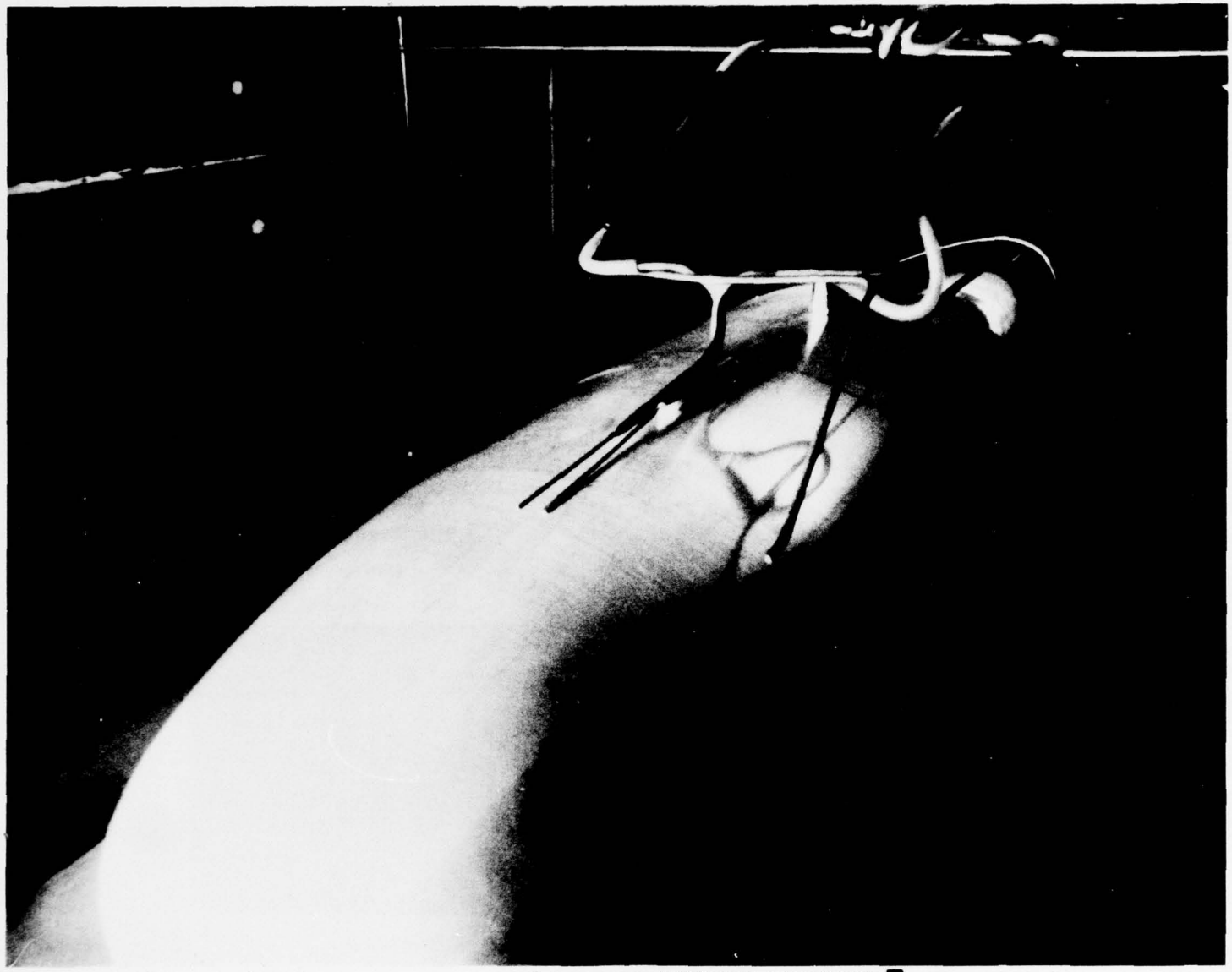

FIGURE 9. SURFACE-TUBE ARRANGEMENT FOR DETECTING TRANSITION

SWEEP SPEED, 2 ms/division

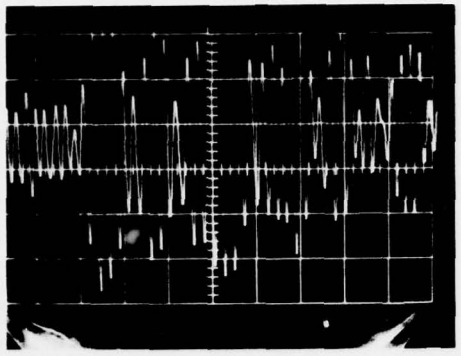

x/R = 1.94

LAMINAR

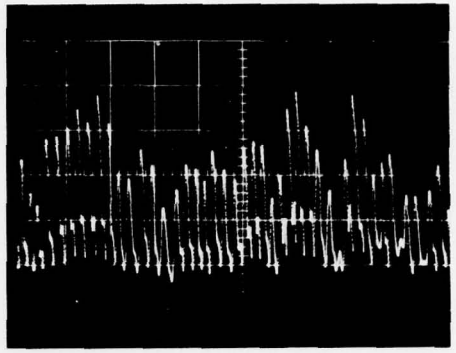

x/R = 2.13

TRANSITIONAL

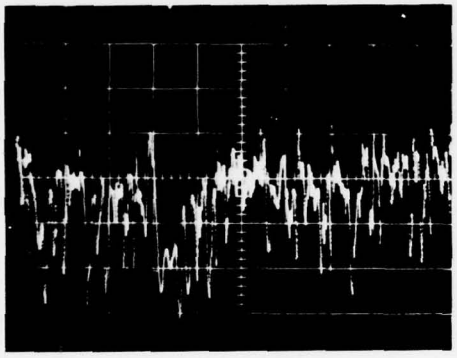

x/R = 2.31

TRANSITIONAL

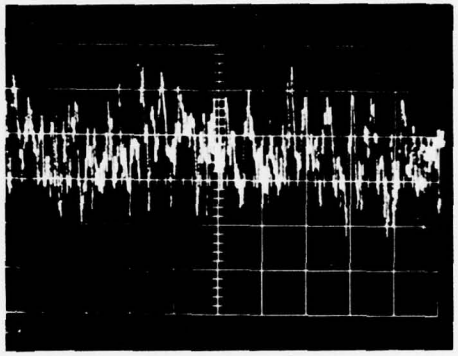

x/R = 2.63

TURBULENT

FIGURE 10. OSCILLOGRAMS OF VELOCITY FLUCTUATIONS ON MODEL B(U_o = 38 m/s)

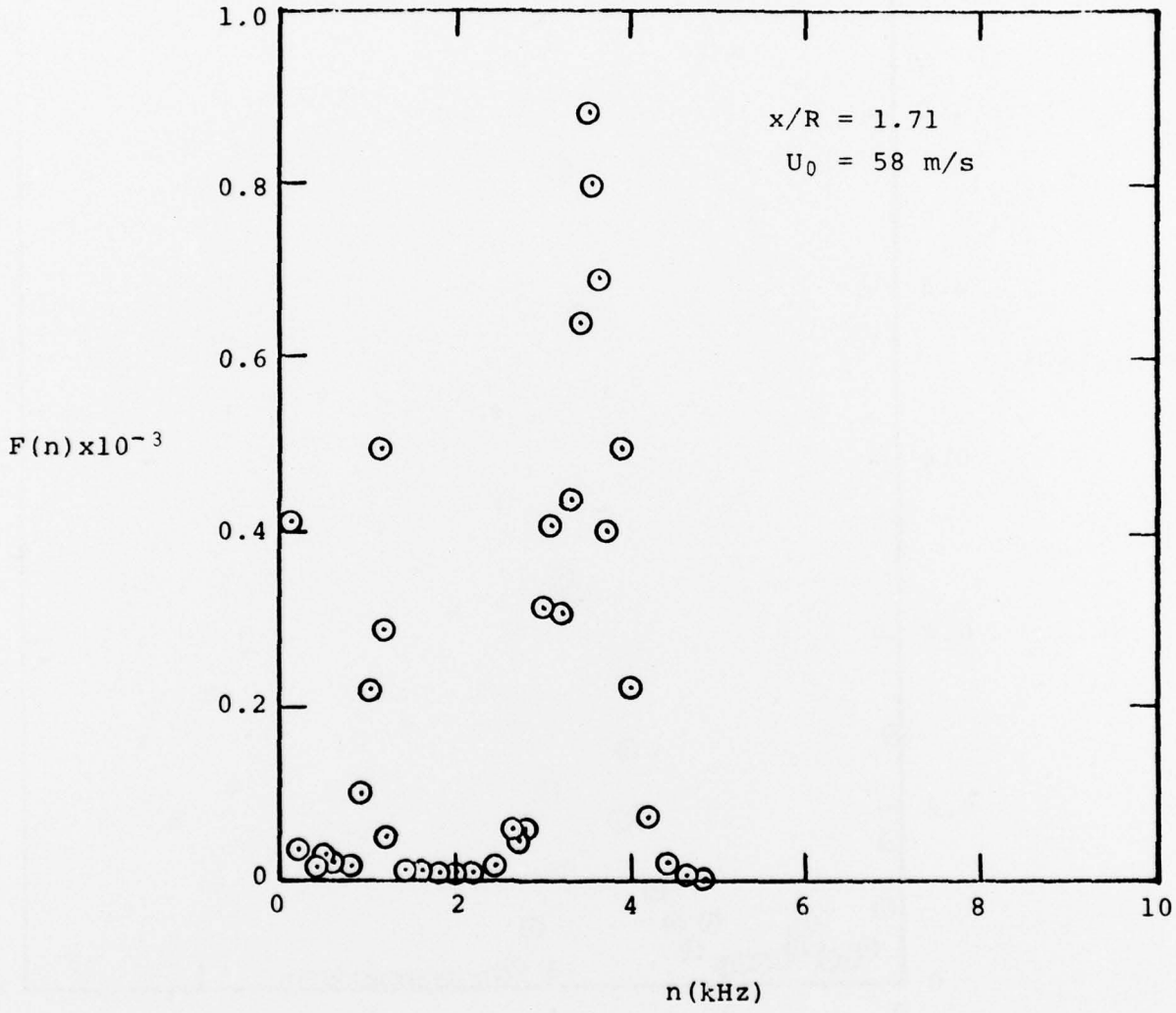

FIGURE 11. Normalized Spectrum, Model B at 0° Angle-of-Attack.

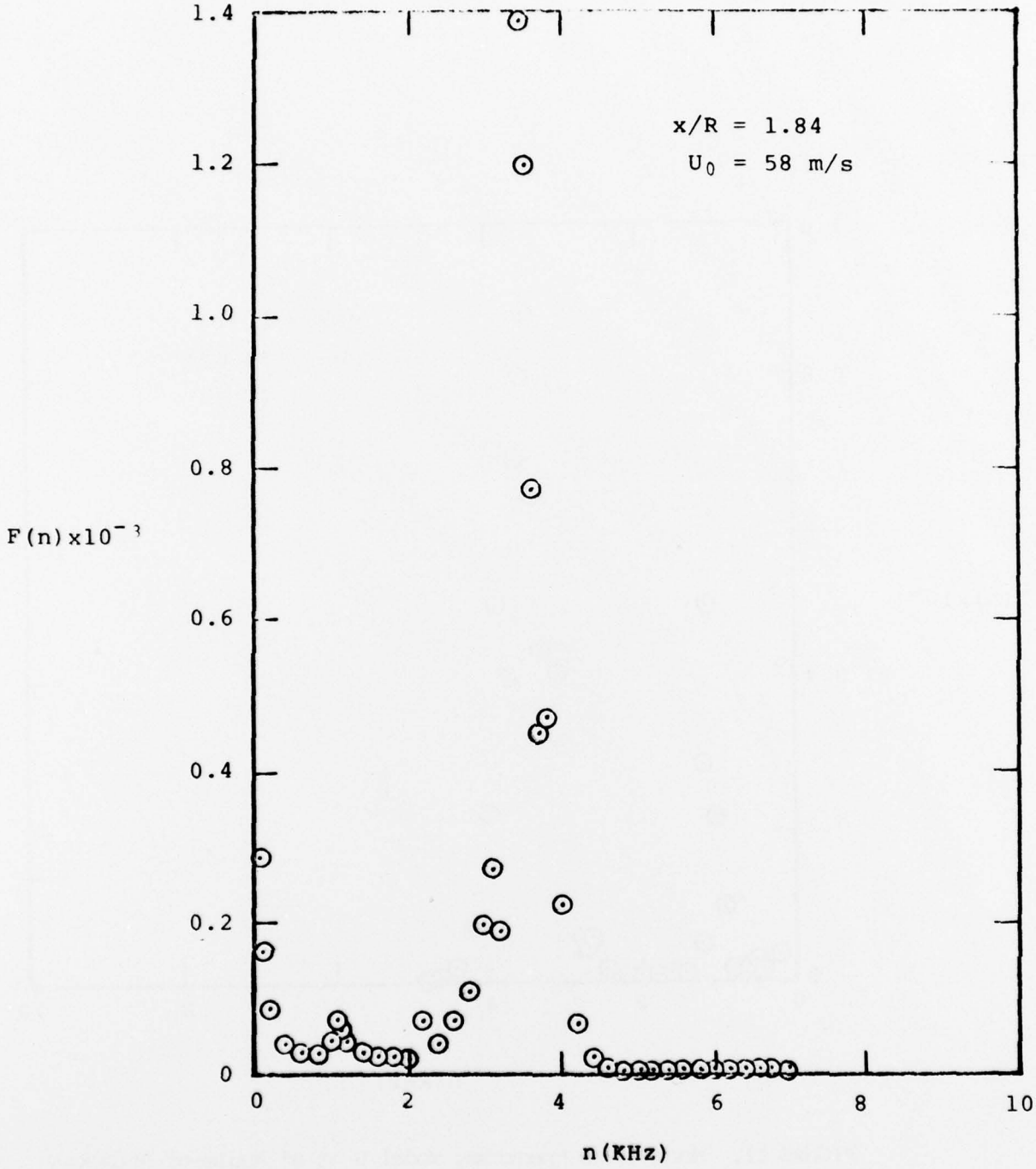

FIGURE 12. Normalized Spectrum, Model B at 0° Angle-of-Attack.

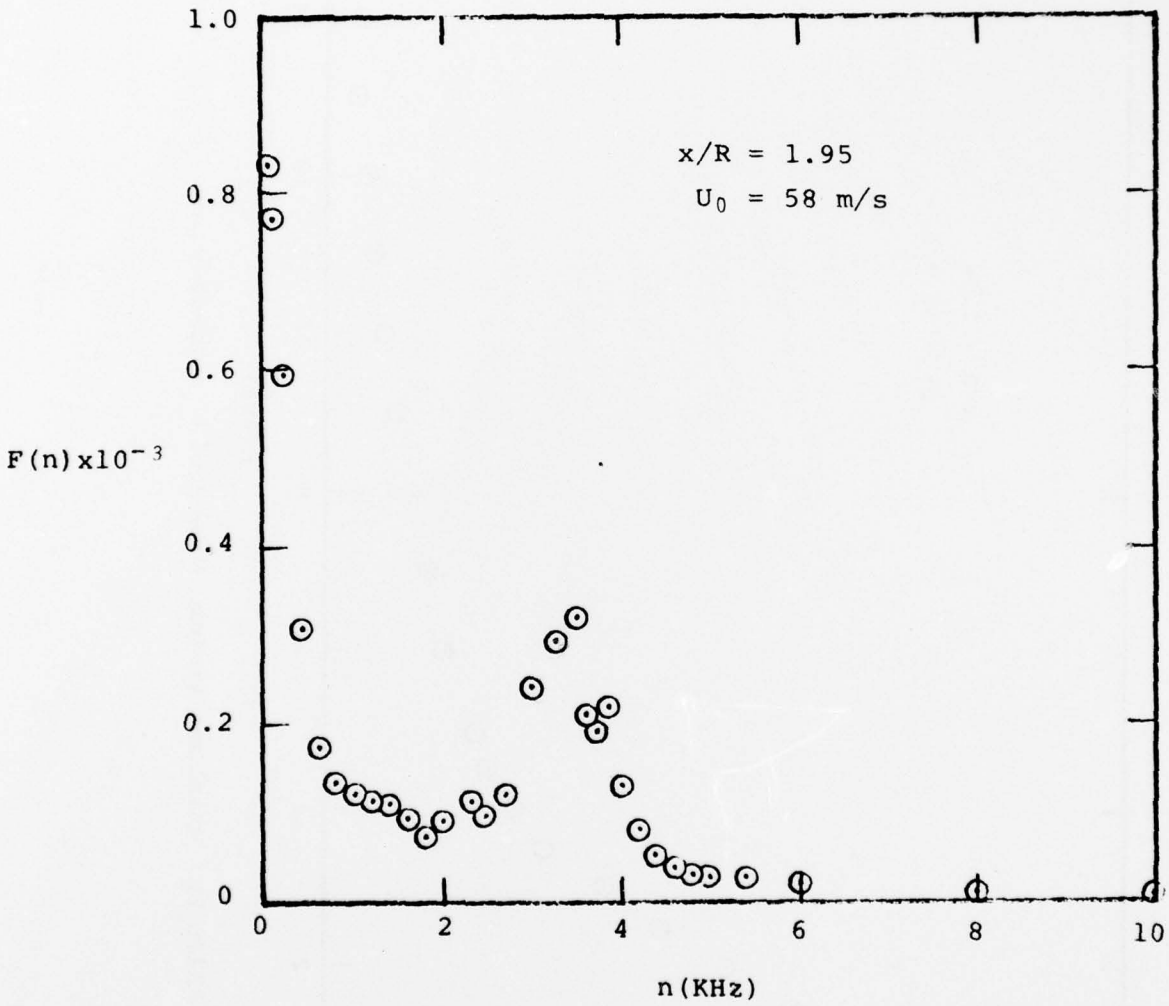

FIGURE 13. Normalized Spectrum, Model B at 0° Angle-of-Attack.

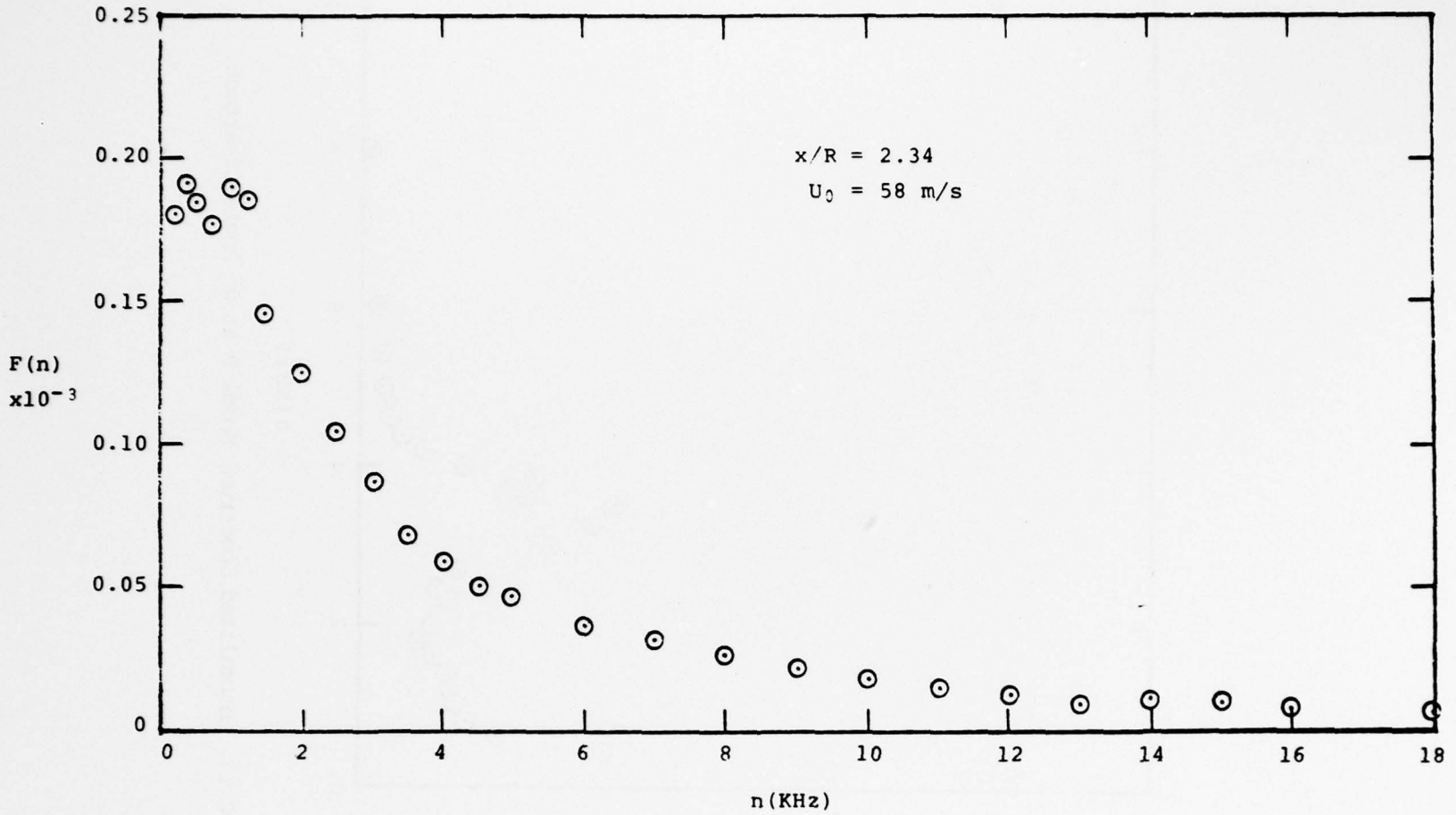

FIGURE 14. Normalized Spectrum, Model B of 0° Angle-of-Attack.

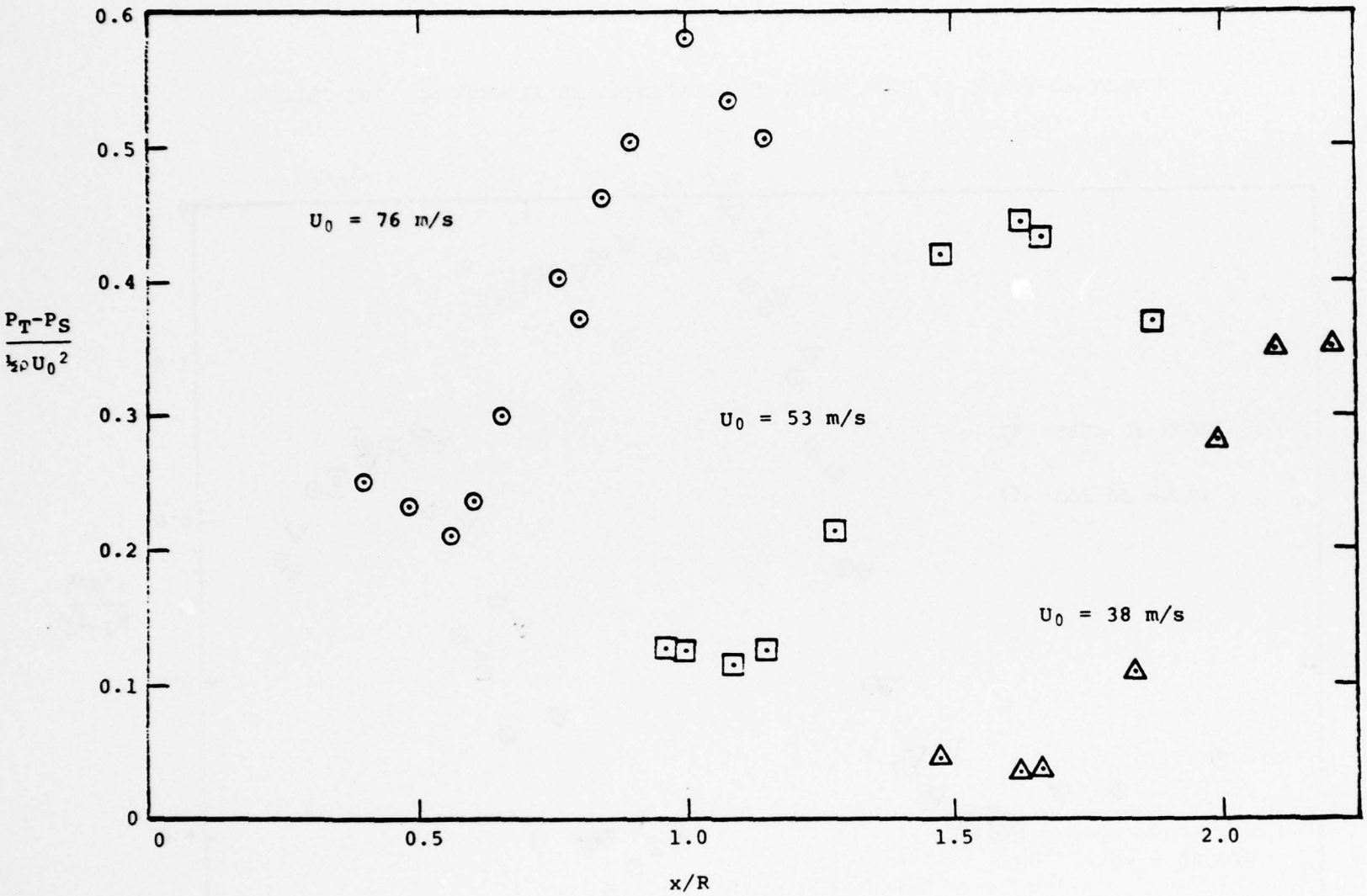

FIG. 15. DETERMINATION OF TRANSITION WITH SURFACE TUBE ON MODEL B AT 3° ANGLE-OF-ATTACK

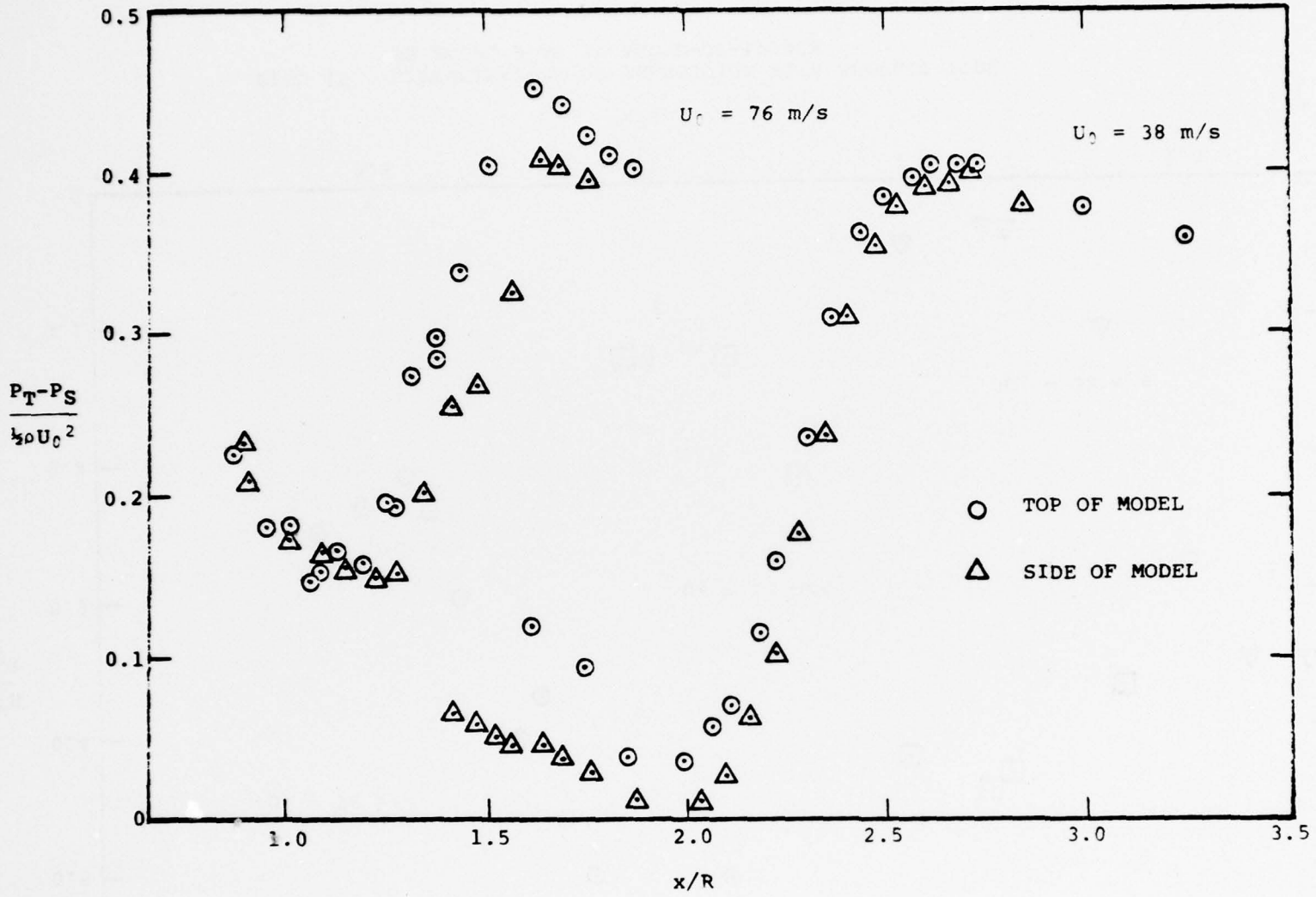

FIG. 16. UNIFORMITY OF TRANSITION ON MODEL B AT 0° ANGLE-OF-ATTACK

NBS-114A (REV. 7-73)

U.S. DEPT. OF COMM. BIBLIOGRAPHIC DATA SHEET	1. PUBLICATION OR REPORT NO. NBSIR-77-1258	2. Gov't Accession No.	3. Recipient's Accession No.
4. TITLE AND SUBTITLE: EXPERIMENTAL STUDY OF TRANSITION ON BLUNT BODIES (PART I)			5. Publication Date: July 1977
			6. Performing Organization Code
7. AUTHOR(S): G. Christoph and K. D. Tidstrom			8. Performing Organ. Report No.
9. PERFORMING ORGANIZATION NAME AND ADDRESS: NATIONAL BUREAU OF STANDARDS, DEPARTMENT OF COMMERCE, WASHINGTON, D.C. 20234			10. Project/Task/Work Unit No. 2130487
			11. Contract/Grant No. PO-4-0011
12. Sponsoring Organization Name and Complete Address (Street, City, State, ZIP): Naval Underwater Systems Center, Newport, Rhode Island 02840			13. Type of Report & Period Covered: Final
			14. Sponsoring Agency Code

15. SUPPLEMENTARY NOTES

16. ABSTRACT (A 200-word or less factual summary of most significant information. If document includes a significant bibliography or literature survey, mention it here.)

Experimental results are presented for the effects of Reynolds number and angle-of-attack on the static pressure distribution and the location of laminar to turbulent transition for the flow over several blunt noseforms; comparisons are made with analytical methods.

17. KEY WORDS (six to twelve entries; alphabetical order; capitalize only the first letter of the first key word unless a proper name; separated by semicolons) Axisymmetric; boundary layer; blunt-nose; hot-wire anemometry; laminar; pressure-distribution; transition; turbulent.

18. AVAILABILITY	19. SECURITY CLASS (THIS REPORT)	21. NO. OF PAGES
[X] Unlimited XX [redacted] [ ] Order From Sup. of Doc., U.S. Government Printing Office Washington, D.C. 20402, SD Cat. No. C13 [ ] Order From National Technical Information Service (NTIS) Springfield, Virginia 22151	UNCLASSIFIED	26
	20. SECURITY CLASS (THIS PAGE) UNCLASSIFIED	22. Price

USCOMM-DC 29042-P74

401299